IEEE Access
Multidisciplinary | Rapid Review | Open Access Journal

Received July 11, 2019, accepted July 29, 2019, date of publication August 1, 2019, date of current version August 14, 2019.

Digital Object Identifier 10.1109/ACCESS.2019.2932330

Iterative Reweighted DOA Estimation for Impulsive Noise Processing Based on Off-Grid Variational Bayesian Learning

FUQIANG MA[1,2,3], CHENG XU[1,2], (Member, IEEE), XIAOTONG ZHANG[1,2,3], (Senior Member, IEEE), JIE HE[1,2], (Member, IEEE), AND WEI SU[2]

[1]Beijing Advanced Innovation Center for Materials Genome Engineering, University of Science and Technology Beijing, Beijing 100083, China
[2]School of Computer and Communication Engineering, University of Science and Technology Beijing, Beijing 100083, China
[3]Beijing Key Laboratory of Knowledge Engineering for Materials Science, Beijing 100083, China

Corresponding authors: Cheng Xu (xucheng@ieee.org) and Xiaotong Zhang (zxt@ies.ustb.edu.cn)

This work was supported in part by the National Key Research and Development Program of China under Grant 2018YFB0704300, in part by the Postdoctoral Innovative Talent Support Program under Grant BX20190033, and in part by the Fundamental Research Funds for the Central Universities under Grant 06500127.

ABSTRACT The performance of acoustic source localization with array system is limited by impulsive noise such as electromagnetic interference, car ignitions, bursting, and so on. The impulsive noise decays with heavy-tailed distribution which can be considered as outliers. In order to alleviate the performance degradation of traditional direction-of-arrival (DOA) estimation with impulsive noise, a novel iterative reweighted variational Bayesian learning algorithm based on off-grid model (OG-WVBL) is proposed. OG-WVBL employs impulsive noise as two independent components and models directly the outliers with sparse distribution in the time domain. OG-WVBL utilizes two iterative VBL to reconstruct signal and outliers matrix and then retrieves the DOA. Then, OG-WVBL also introduces the iteratively reweighted strategy to hyperparameters so that the more importance is given to those hyperparameters with non-zero entries over others which can encourage sparsity and achieve the consistent convergence. With the iteratively reweighted strategy, OG-WVBL can automatically identify the number of sources without any prior knowledge. Moreover, the proposed algorithm can use a coarse sampling grid to achieve the accurate DOA estimation with the off-grid model. The experiments and simulation results show that OG-WVBL possesses robust performance and outperforms several existing algorithms under impulsive noise environment.

INDEX TERMS DOA estimation, iterative reweighted, variational Bayesian learning, impulsive noise, off-grid.

I. INTRODUCTION

The direction-of-arrival (DOA) estimation of multiple narrowband sources is one of the main issues in the field of array signal processing with tremendous applications, such as radio communication, radar, sonar, seismic detection, acoustic source localization [1]–[4] and so on. At present, acoustic source localization is widely applied in military and civilian fields. In the military field, DOA estimation can not only track vehicles, aircraft and other targets which are located in the blind area of radar, but also detect the snipers in real time. DOA estimation can also be exploited to video conferencing system and intelligent transportation, such as monitoring whistles of car.

The conventional subspace-based DOA estimation algorithms, such as MUSIC and ESPRIT [5], [6], can provide high resolution with the Gaussian noise assumption. Many existing DOA estimations are also based on the assumption that the noise obeys Gaussian distribution [7]. Since the Gaussian distribution has any order statistics, the traditional DOA approaches can effectively achieve the accurate estimation according to second-order statistics [8]. However, because of atmospheric noise, electromagnetic interference, car ignitions, instantaneous attack of heavy objects, equipment noise, and bursting in practical environments, the acoustic signal is usually corrupted by extremely impulsive noise

The associate editor coordinating the review of this manuscript and approving it for publication was Mingjian Li.

that exhibits irregularity in time domain. In addition, the probability density functions (pdf) of impulsive noise decay with heavy tails and do not follow common Gaussian properties [9]. Impulsive noise possesses the characteristics of large amplitudes and short duration. The large amplitudes of heavy tails can be considered as outliers which have a higher probability of occurrence. Thus, those outliers exceed the standard deviations than Gaussian distribution [10], [11]. The traditional DOA estimations may fail in the presence of non-Gaussian noise which does not have finite second-order statistics. In order to deal with the heavy-tailed distribution, several impulsive noise models have been proposed, that is, Gaussian mixture model (GMM) [11], generalized Gaussian distribution (GGD) [12], α-stable distribution [13], and Student-t distribution [14].

Many robust DOA estimation algorithms have been proposed to alleviate the effect of impulsive noise. The maximum likelihood (ML) method uses GMM noise to estimate DOA [15]. ML method is a complicated nonlinear and nonconvex multi-dimensional optimization which leads to a heavy computational complexity. Furthermore, because α-stable distribution with $\alpha \neq 1$ and $\alpha \neq 2$ does not have a closed-form expression of pdf, ML will fail to solve it. l_p-MUSIC algorithm minimizes the unconstrained l_p-norm of the residual error matrix instead of the Frobenius norm. It adopts the alternating convex optimization to get a closed-form expression [11]. The efficient solutions are designed in time domain without explicitly constructing the covariance. Although l_p-norm is robust to outliers with $1 \leq l_p < 2$, it requires the accurate number of source.

A class of fractional lower-order statistics (FLOS) algorithms exhibits a more robust performance than second order statistics for impulsive noise. Those algorithms based FLOS include the robust covariation in ROC-MUSIC [16], the fractional lower-order moments (FLOM) based MUSIC [17] and the phased fractional lower-order moments (PFLOM) based MUSIC [18]. However, they are suboptimal which depend on the relationship between the parameter of FLOS and the characteristic exponent of α-stable distribution. The zero-memory nonlinear (ZMNL) functions [19] have been used to suppress impulsive noise by restrain the amplitude of outliers and achieve more accurate DOA estimations than FLOS based algorithms. This method leads to lose the potential information of signal and destroys the low-rank property of the subspace.

The relevant statistics use a robust kernel function to solve impulsive noise [20]. The advantage of relevant statistics, such as the M-estimator [10], S-estimator, or MM-estimator [21] is exploited to construct the covariance matrix which is less sensitive to impulsive noise. Then, the conventional MUSIC algorithm can be applied to get the DOA estimations. This representative approach is similar to the fractional lower-order statistics algorithm.

Another effective DOA estimation is based on the sparse representation [22]–[24]. Because DOA of sources is sparse relative to the whole spatial domain, the sparse representation methods possess many advantages compared to the traditional subspace based methods, such as the sparse representation of array covariance vector (SRACV) [25]. The sparse representation methods can deal with correlated sources and small snapshots and are robust against noise. Sparse Bayesian learning (SBL) [26]–[31] is widely used in the sparse array signal processing, which exploits the sparse recovery with a sparse prior assumption from Bayesian inference. Compared with the conventional Basis Pursuit (BP) [32], SBL can achieve the globally optimal solution only with a few local minimum values. Under the framework of SBL, Yang [33] proposed an off-gird sparse Bayesian inference algorithm (OGSBI), which can accurately estimate DOA with rough grid intervals when the true DOA dose not locate at the discretized grid. At the same time, OGSBI employs the singular value decomposition (SVD) to relieve the computational complexity which makes it suitable for the multi-snapshot scenario as well as single snapshot. Yang [34] also proposed a Sparse Parametric Approach (SPA), which estimates the sparse parameters in a continuous range based on the array covariance fitting and convex optimization criterion. Dai [35] [46] used the root of certain polynomial to solve the off-gird problem and achieved high accuracy DOA estimation with low computational complexity. OGSBL [46] can effectively suppress impulsive noise, but it can not achieve the consistent convergence of hyperparameters which employ the same prior distribution. When impulsive noise has heavy tails or GSNR is low, the number of signal sources may not be accurately estimated. OGSBL uses the marginal likelihood function to estimate sparse vectors, which has slow convergence speed. The variational Bayesian learning (VBL) [41]–[44] can provide effective estimation for the distributions of unknown deterministic parameters, which can effectively reduce the complexity and avoid calculating the marginal distribution. The variational expectation-maximization algorithm [45] takes advantage of a Gaussian-Wishart hierarchical prior to solve the problem of low-rank phase retrieval which is less sensitive to the choice of the initialization point. In order to effectively analyze the performance of SBL, the Cramer-Rao lower bound (CRLB) is derived [36].

Because the traditional VBL and OGSBI algorithms are incapable of dealing with impulsive noise directly and based on a unified assumption with respect to the hyperparameters which is difficult to identify the number of sources, we propose a iterative reweighted variational Bayesian learning algorithm based on the off-grid model (OG-WVBL) to effectively alleviate impulsive noise. OG-WVBL employs impulsive noise with heavy-tailed distribution as two independent components in the context of multiple measurement vectors (MMV), and models directly the outliers with sparse distribution in time domain. Thus, the signal and outliers matrix can be regarded as employing the same Gaussian prior distribution. OG-WVBL utilizes two iterative VBL to reconstruct signal and outliers matrix and then retrieves the DOA. In order to solve the inconsistent

convergence of OGSBL [46], OG-WVBL also introduces the iterative reweighted strategy to hyperparameters so that the more importance is given to those hyperparameters with non-zero entries over others which can encourage sparsity. The reweighted vector and VBL are updated alternately to promote convergence. With the iterative reweighted strategy, OG-WVBL can automatically identify the number of sources without any prior knowledge. Moreover, the proposed algorithm can use a coarse sampling grid to achieve the accurate DOA estimation with off-grid model. The OG-WVBL is compared in performance with CRLB. In summary, OG-WVBL is also convenient to implement which gives it an edge in DOA estimation performance.

The main contributions of this paper can be summarized as follows:

1) The reweighted vector can promote convergence speed of OG-WVBL, and ensures that OG-WVBL can accurately estimate the number of sources without requiring the prior knowledge of sources.
2) OG-WVBL brings a much small RMSE in low GSNR with the reweighted vector and ensures the row sparsity of signal as well as its satisfactory performance.
3) The prominent superiority is capable of identifying the location and amplitude of impulsive noise.
4) The distribution of impulsive noise in truck environment is counted and the validity of OG-WVBL is verified by truck data.

This paper is organized as follows. In Section II, we analyze the statistical model of impulsive noise and signal model. In Section III, we propose the robust off-grid DOA estimation for impulsive noise processing based on weighted variational Bayesian learning and analyze its performance. Section IV shows experiments and simulation results. Finally, Section V concludes this paper.

In the paper, we make full use of the following notations. $(\cdot)^{\mathrm{T}}$, $(\cdot)^{\mathrm{H}}$ denote the transpose and Hermitian transpose, respectively. we define $diag(\cdot)$ is a diagonal matrix. $E[\cdot]$ represents expectation operator. $\Re\{\cdot\}$ represents the real part of variable. $\odot$ denotes the Hadamard product. tr$(\cdot)$ is the trace of a matrix.

II. STATISTICAL MODEL OF IMPULSIVE NOISE AND SIGNAL MODEL

A. IMPULSIVE NOISE MODEL UNDER TRUCK ENVIRONMENT

Several statistical models have been researched to indicate the temporal and spatial properties of impulsive noise such as α-stable distribution. Nikias [13] described impulsive noise of atmospheric caused by thunder and lightning with α-stable distribution. Bian [37] proved that the sea clutter possesses non-Gaussian distribution in sonar applications and can be described by α-stable distribution. Xiao [38] analyzed the characteristics of acoustic impulsive noise. The periodic impulsive noise in narrowband powerline communications [39] bears the sparsity in time domain and is estimated by sparse Bayesian learning.

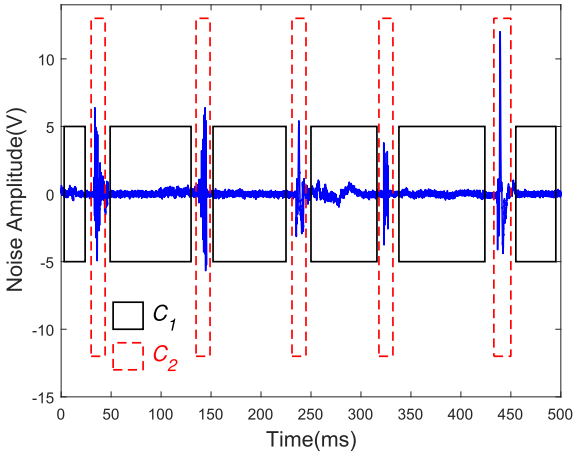

FIGURE 1. The time plot of impulsive noise under truck environment.

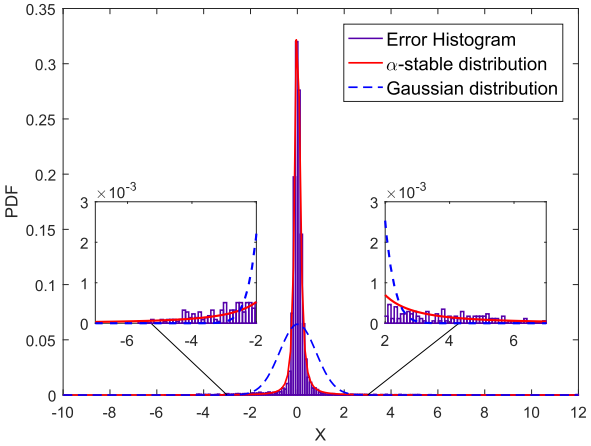

FIGURE 2. The estimated probability density function of impulsive noise.

In this section, we analyze the statistical model of impulsive noise under truck environment. Many acoustic noises are instantaneous in practical environment. We use the microphone array system to collect impulsive noise in the city, such as the noise of machine, equipment startup, thunder, instantaneous attack of heavy objects, blast of wind, and so on. From Fig.1, noise can be partitioned into two stationary intervals C_1 and C_2. The interval C_1 can be regarded as normal noise with a stationary Gaussian process. The interval C_2 can be considered as outliers with large amplitudes. The proportion of interval C_2 is very small in the whole time domain. Therefore, the outliers possess sparse properties which be considered as heavy tails of pdf. One of the goals is to identify the location and amplitude of impulsive noise. Fig.2 shows the estimated pdf of impulsive noise. The blue histogram represents the true error distribution of impulsive noise. The red curve is α-stable distribution and the blue curve is Gaussian distribution. Gaussian distribution deviates from the true error distribution even if around zero. However, α-stable distribution can fit the true error distribution. When error ranges between two and six, α-stable distribution can

also effectively indicate error. Therefore, α-stable distribution provides a powerful model estimation for acoustics impulsive noise.

B. ARRAY SIGNAL MODEL

It is considered that a uniform linear array of M isotropic sensors receives the far field signal generated by P uncorrelated narrowband sources. The P sources impinging on the array from directions $\boldsymbol{\theta} = [\theta_1, \theta_2, \cdots, \theta_P]$ with powers σ_p^2, $p = 1, 2, \cdots, P$. Note that the first element is the reference sensor. $s_p(t)$ is the complex envelope of pth source at time t, $t = 1, 2, \cdots, T$. Then, the $M \times 1$ signal vector $\boldsymbol{x}(t) = [x_1(t), \cdots, x_m(t), \cdots, x_M(t)]$, $m = 1, 2, \cdots, M$ can be modeled as [11]:

$$\begin{aligned}\boldsymbol{x}(t) &= \sum_{p=1}^{P} \boldsymbol{a}(\theta_p)s_p(t) + \boldsymbol{n}(t) = \boldsymbol{A}(\boldsymbol{\theta})\boldsymbol{s}(t) + \boldsymbol{n}(t) \\ &= \boldsymbol{A}(\boldsymbol{\theta})\boldsymbol{s}(t) + \boldsymbol{w}(t) + \boldsymbol{e}(t) \quad (1)\end{aligned}$$

$$\boldsymbol{a}(\theta_p) = [1, \mathrm{e}^{-j2\pi d \sin\theta_p/\lambda}, \cdots, \mathrm{e}^{-j2\pi d(M-1)\sin\theta_p/\lambda}]^{\mathrm{T}} \quad (2)$$

where $\boldsymbol{a}(\theta_p)$ is a $M \times 1$ steering vector of the array corresponding to direction θ_p and λ is wavelength of signal. $\boldsymbol{A}(\boldsymbol{\theta}) = [\boldsymbol{a}(\theta_1), \boldsymbol{a}(\theta_2), \cdots, \boldsymbol{a}(\theta_P)]$ is a $M \times P$ array manifold, $\boldsymbol{s}(t) = [s_1(t), s_2(t), \cdots, s_P(t)]^{\mathrm{T}}$ is a $P \times 1$ source vector at time t, $\boldsymbol{n}(t) = [n_1(t), n_2(t), \cdots, n_M(t)]^{\mathrm{T}}$ is a $M \times 1$ impulsive noise vector, and they are all independent of each other and uncorrelated with the sources. The heavy-tailed noise can be naturally divided into mutually independent components [39]. $\boldsymbol{w}(t)$ is the component of outliers which involves the impulsive amplitude, and $\boldsymbol{e}(t)$ is a dense Gaussian noise vector with zero-mean independent and identically distributed (IID) entries. Note that the non-zero entities of $\boldsymbol{w}(t)$ are greater than that of $\boldsymbol{e}(t)$, and $\boldsymbol{w}(t)$ is a sparse vector where most of entities are zero. In practice, the received signal model (1) can also be rewritten as (3) by using the T available samples:

$$\boldsymbol{X} = \boldsymbol{A}(\boldsymbol{\theta})\boldsymbol{S} + \boldsymbol{N} = \boldsymbol{A}(\boldsymbol{\theta})\boldsymbol{S} + \boldsymbol{W} + \boldsymbol{E} \quad (3)$$

where

$$\begin{aligned}\boldsymbol{X} &= [\boldsymbol{x}(1), \boldsymbol{x}(2), \cdots, \boldsymbol{x}(T)] \\ \boldsymbol{S} &= [\boldsymbol{s}(1), \boldsymbol{s}(2), \cdots, \boldsymbol{s}(T)] \\ \boldsymbol{N} &= [\boldsymbol{n}(1), \boldsymbol{n}(2), \cdots, \boldsymbol{n}(T)] \\ \boldsymbol{W} &= [\boldsymbol{w}(1), \boldsymbol{w}(2), \cdots, \boldsymbol{w}(T)] \\ \boldsymbol{E} &= [\boldsymbol{e}(1), \boldsymbol{e}(2), \cdots, \boldsymbol{e}(T)] \quad (4)\end{aligned}$$

where $\boldsymbol{X}$ is the $M \times T$ matrix of the sources received by the array sensors. $\boldsymbol{S}$ is the $P \times T$ matrix of the sources. There is an assumption that the number M of the array elements is greater than the number P of the sources.

We also re-derive the off-grid model [33] by using first-order Taylor series expansion and it can provide a suboptimal array manifold compared with the on-grid one. The potential spatial domain is discretized as a fixed sampling grid $\hat{\boldsymbol{\theta}} = \{\hat{\theta}_1, \hat{\theta}_2, \cdots, \hat{\theta}_N\}$ with the DOA range $[-\pi/2, \pi/2]$, and N represents the grid number which typically satisfies $N \gg M$. At the same time, sampling grid $\hat{\boldsymbol{\theta}}$ is a $r = \hat{\theta}_2 - \hat{\theta}_1 = \pi/(N-1)$ uniform angular interval. If $\theta_p \notin \{\hat{\theta}_1, \hat{\theta}_2, \cdots, \hat{\theta}_N\}$ for some $p \in \{1, 2, \cdots, P\}$, $\hat{\theta}_{n_p}$, $n_p \in \{1, 2, \cdots, N\}$, is the nearest grid point to the true direction θ_p. We derives the steering vector $\boldsymbol{a}(\theta_p)$ from first-order Taylor series expansion:

$$\boldsymbol{a}(\theta_p) \approx \boldsymbol{a}(\hat{\theta}_{n_p}) + \boldsymbol{b}(\hat{\theta}_{n_p})(\theta_p - \hat{\theta}_{n_p}) \quad (5)$$

where $\boldsymbol{b}(\hat{\theta}_{n_p})$ is the derivative of $\boldsymbol{a}(\hat{\theta}_{n_p})$. $\boldsymbol{A} = [\boldsymbol{a}(\hat{\theta}_1), \boldsymbol{a}(\hat{\theta}_2), \cdots, \boldsymbol{a}(\hat{\theta}_N)]$ is the primary on-grid array manifold, $\boldsymbol{B} = [\boldsymbol{b}(\hat{\theta}_1), \boldsymbol{b}(\hat{\theta}_2), \cdots, \boldsymbol{b}(\hat{\theta}_N)]$ is the derivative matrices of $\boldsymbol{A}$, $\boldsymbol{\beta} = [\beta_1, \beta_2, \cdots, \beta_N] \in [-\frac{1}{2}r, \frac{1}{2}r]^N$ is the bias of grid and $\boldsymbol{\Phi}(\boldsymbol{\beta}) = \boldsymbol{A} + \boldsymbol{B}diag(\boldsymbol{\beta})$ is the off-grid array manifold.

$$\begin{aligned}\beta_n &= \theta_p - \hat{\theta}_{n_p}, \\ \hat{s}_n(t) &= s_{n_p}(t), \quad \text{if } n = n_p \quad \text{for any} \quad p \in \{1, 2, \cdots, P\}; \\ \beta_n &= 0, \quad \hat{s}_n(t) = 0, \ otherwise \quad (6)\end{aligned}$$

When the approximation error aligns to the measurement noise, the signal model in (1) and (3) can be modeled as:

$$\begin{aligned}\boldsymbol{x}(t) &= \boldsymbol{\Phi}(\boldsymbol{\beta})\hat{\boldsymbol{s}}(t) + \boldsymbol{n}(t) \\ &= \boldsymbol{\Phi}(\boldsymbol{\beta})\hat{\boldsymbol{s}}(t) + \boldsymbol{w}(t) + \boldsymbol{e}(t) \quad (7) \\ \boldsymbol{X} &= \boldsymbol{\Phi}(\boldsymbol{\beta})\hat{\boldsymbol{S}} + \boldsymbol{W} + \boldsymbol{E} \quad (8)\end{aligned}$$

It should be noted that the off-grid dictionary in (7) is closely consistent with the primary on-grid one if $\boldsymbol{\beta} = \boldsymbol{0}$. As a consequence, the off-grid model has a much smaller estimation error than the on-grid one. On the other hand, coarser sampling intervals can effectively reduce computational complexity with comparable modeling accuracy.

III. OFF-GRID ITERATIVE REWEIGHTED VARIATIONAL BAYESIAN LEARNING

In the presence of outliers matrix $\boldsymbol{W}$, the pdf of $\boldsymbol{n}(t)$ has heavier tails than the Gaussian distribution, which will have a few large outliers. In order to achieve the robustness of DOA estimation, we need to not only estimate the sparse signals $\hat{\boldsymbol{s}}(t)$, $t = 1, 2, \cdots, T$, but also identify the sparse outliers $\boldsymbol{W}$. To mitigate impulsive noise, we exploit the DOA problem in time domain based on the iterative reweighted variational Bayesian learning methods, and apply a fixed-point iteration approach to jointly estimate $\hat{\boldsymbol{S}}$ and $\boldsymbol{W}$. In this paper, to achieve the robustness of OG-WVBL, we assign different parameters of Gamma distribution to hyperparameters, and give more importance to some hyperparameters over others.

A. UPDATE $\hat{S}$ PROCEDURE FOR OG-WVBL

The model of iterative reweighted variational Bayesian learning is shown as Fig.3. We update the hidden variable $\hat{\boldsymbol{S}}$ while considering the outliers matrix $\boldsymbol{W}$ as a fixed sparse matrix. The signal model is represented as:

$$\bar{\boldsymbol{X}} = \boldsymbol{X} - \boldsymbol{W} = \boldsymbol{\Phi}(\boldsymbol{\beta})\hat{\boldsymbol{S}} + \bar{\boldsymbol{E}} \quad (9)$$

$\bar{\boldsymbol{X}}$ is the optimized observation which does not contain the outliers $\boldsymbol{W}$. $\bar{\boldsymbol{E}}$ that is equivalent to $\boldsymbol{E}$ is a white complex

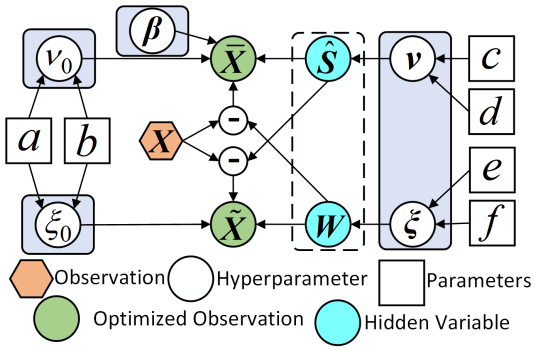

FIGURE 3. The iterative model of reweighted variational Bayesian learning.

Gaussian noise with zero-mean independent and identically distributed (IID) entries:

$$p(\bar{\boldsymbol{E}}|\nu_0) = \prod_{t=1}^{T} CN(\boldsymbol{e}(t)|\boldsymbol{0}, \nu_0^{-1}\boldsymbol{I}) \tag{10}$$

where $\nu_0 = \sigma^{-2}$ denotes the noise precision, and σ^2 is the noise variance. Then, $p(\bar{\boldsymbol{X}}|\hat{\boldsymbol{S}}, \nu_0, \boldsymbol{\beta})$ also follows complex Gaussian distribution.

$$p(\bar{\boldsymbol{X}}|\hat{\boldsymbol{S}}, \nu_0, \boldsymbol{\beta}) = \prod_{t=1}^{T} CN(\bar{\boldsymbol{x}}(t)|\boldsymbol{\Phi}(\boldsymbol{\beta})\hat{\boldsymbol{s}}(t), \nu_0^{-1}\boldsymbol{I}) \tag{11}$$

The hyperparameter ν_0 is usually unknown in practice. A Gamma hyperprior is used for ν_0:

$$p(\nu_0; a, b) = \Gamma(\nu_0|a, b) \tag{12}$$

where $\Gamma(\nu_0|a, b) = [\Gamma(a)]^{-1}b^a\nu_0^{a-1}\exp(-b\nu_0)$ and $\Gamma(\cdot)$ is Gamma function which is used as a conjugate prior distribution of VBL. Parameter a is the shape parameter, and b is the scale parameter of Gamma distribution. The parameter influences how the pdf is concentrated. The pdf will be concentrated around zero if parameter a reach a small value, otherwise; the PDF is concentrated around its single mode (i.e., $\frac{a-1}{b}$) with large values of a. In addition, the larger the parameter b, the narrower the pdf.

Following the VBL principle, $\hat{\boldsymbol{S}}$ is a row sparse matrix, and we assume that $\hat{\boldsymbol{S}}$ follows the complex Gaussian prior for each $\hat{\boldsymbol{s}}(t)$. We have two-stage hierarchical prior with hyperparameters vector $\boldsymbol{\nu}$:

$$p(\hat{\boldsymbol{S}}|\boldsymbol{\nu}) = \prod_{t=1}^{T} CN(\hat{\boldsymbol{s}}(t)|\boldsymbol{0}, \boldsymbol{\Lambda}^{-1}) \tag{13}$$

where $\boldsymbol{\nu} = [\nu_1, \nu_2, \cdots, \nu_N]^{\mathrm{T}}$ and $\boldsymbol{\Lambda} = diag(\boldsymbol{\nu})$. All columns of $\hat{\boldsymbol{S}}$ are independent and the hyperparameter ν_n is modeled as independent Gamma distribution. For a larger ν_n, $\hat{s}_i(t)$ has a smaller variance with high probability $\hat{s}_i(t)$ being zero. In order to keep in line with characteristic of row sparsity, we assign different parameters of Gamma distribution to hyperparameters $\boldsymbol{\nu}$ corresponding to apply different weights to different row vectors of the sparse matrix $\hat{\boldsymbol{S}}$. The iterative reweighted VBL turns out to be more importance for some hyperparameters over others, and make robust estimation of desired signal direction $\boldsymbol{\theta}$. Because it is the conjugate prior for the precision of a univariate Gaussian. The independent Gamma hyperprior of $\boldsymbol{\nu}$ with different parameters c_n, d_n can be modeled as:

$$p(\boldsymbol{\nu}; \boldsymbol{c}, \boldsymbol{d}) = \prod_{n=1}^{N} \Gamma(\nu_n|c_n, d_n) \tag{14}$$

A uniform prior is assumed for $\boldsymbol{\beta}$:

$$\boldsymbol{\beta} \sim U([-\frac{1}{2}r, \frac{1}{2}r]^N) \tag{15}$$

On the basis of Bayes' rule in Fig.3, the joint probability function of all parameters combined with the above probability distribution (12), (13), (14), (15) is

$$p(\bar{\boldsymbol{X}}, \hat{\boldsymbol{S}}, \nu_0, \boldsymbol{\nu}, \boldsymbol{\beta}) = p(\bar{\boldsymbol{X}}|\hat{\boldsymbol{S}}, \nu_0, \boldsymbol{\beta})p(\hat{\boldsymbol{S}}|\boldsymbol{\nu})p(\boldsymbol{\nu})p(\nu_0)p(\boldsymbol{\beta}) \tag{16}$$

Consider a probabilistic model with the optimized observation $\bar{\boldsymbol{X}}$, hidden variables $\hat{\boldsymbol{S}}$, the unknown deterministic hyperparameters $\boldsymbol{\Theta}_0 = \{\nu_0, \boldsymbol{\nu}, \boldsymbol{\beta}\}$, $\boldsymbol{\Theta} = \{\hat{\boldsymbol{S}}, \boldsymbol{\Theta}_0\}$. According to variational Bayesian inference, the probability distribution $\bar{\boldsymbol{X}}$ can be decomposed into two independent terms with an arbitrary probability density function $q(\boldsymbol{\Theta})$ [41]:

$$\begin{aligned} \ln(p(\bar{\boldsymbol{X}})) &= \int q(\boldsymbol{\Theta})\ln(p(\bar{\boldsymbol{X}}))\mathrm{d}\boldsymbol{\Theta} \\ &= \ln\frac{p(\bar{\boldsymbol{X}}, \boldsymbol{\Theta})}{q(\boldsymbol{\Theta})} - \ln\frac{p(\boldsymbol{\Theta}|\bar{\boldsymbol{X}})}{q(\boldsymbol{\Theta})} \\ &= L(q(\boldsymbol{\Theta})) + KL(q(\boldsymbol{\Theta})|p(\boldsymbol{\Theta}|\bar{\boldsymbol{X}})) \end{aligned} \tag{17}$$

where

$$L(q(\boldsymbol{\Theta})) = \int q(\boldsymbol{\Theta})\ln\frac{p(\bar{\boldsymbol{X}}, \boldsymbol{\Theta})}{q(\boldsymbol{\Theta})}\mathrm{d}\boldsymbol{\Theta} \tag{18}$$

and

$$KL(q(\boldsymbol{\Theta})|p(\boldsymbol{\Theta}|\bar{\boldsymbol{X}})) = -\int q(\boldsymbol{\Theta})\ln\frac{p(\boldsymbol{\Theta}|\bar{\boldsymbol{X}})}{q(\boldsymbol{\Theta})}\mathrm{d}\boldsymbol{\Theta} \tag{19}$$

$KL(q(\boldsymbol{\Theta})|p(\boldsymbol{\Theta}|\bar{\boldsymbol{X}}))$ is the Kullback-Leibler divergence which indicates the similarity between the probability distribution $q(\boldsymbol{\Theta})$ and the posterior distribution $p(\boldsymbol{\Theta}|\bar{\boldsymbol{X}})$. The smaller the Kullback-Leibler divergence, the higher the similarity between $q(\boldsymbol{\Theta})$ and $p(\boldsymbol{\Theta}|\bar{\boldsymbol{X}})$. The log-likelihood function $\ln p(\bar{\boldsymbol{X}})$ is only related to the optimized observation $\bar{\boldsymbol{X}}$, which is unaffected by parameters $\boldsymbol{\Theta}$. Since $KL(q(\boldsymbol{\Theta})|p(\boldsymbol{\Theta}|\bar{\boldsymbol{X}})) \geq 0$, $L(q(\boldsymbol{\Theta}))$ is a lower bound on $\ln(p(\bar{\boldsymbol{X}}))$. When the probability distribution $q(\boldsymbol{\Theta})$ equals the posterior distribution $p(\boldsymbol{\Theta}|\bar{\boldsymbol{X}})$, $L(q(\boldsymbol{\Theta}))$ achieves maximum. Because $KL(q(\boldsymbol{\Theta})|p(\boldsymbol{\Theta}|\bar{\boldsymbol{X}}))$ bears on the posterior distribution $p(\boldsymbol{\Theta}|\bar{\boldsymbol{X}})$ which does not have the closed-form expression, it is usually difficult to directly minimize the Kullback-Leibler divergence $KL(q(\boldsymbol{\Theta})|p(\boldsymbol{\Theta}|\bar{\boldsymbol{X}}))$. To solve this problem, we alternatively maximize its lower bound $L(q(\boldsymbol{\Theta}))$. Therefore, VBL alternatively maximizes $L(q(\boldsymbol{\Theta}))$ with respect to $q(\hat{\boldsymbol{S}})$ and $q(\boldsymbol{\Theta}_0)$

by using EM methodology. First, the current probability distribution $q^{old}(\boldsymbol{\Theta}_0)$ of hyperparameters $\boldsymbol{\Theta}_0$ is fixed, the hidden variables $\hat{\boldsymbol{S}}$ is updated by maximizing $L(q(\hat{\boldsymbol{S}}), q^{old}(\boldsymbol{\Theta}_0))$, which is regarded as the maximization step. Then, the current hidden variables $\hat{\boldsymbol{S}}^{old}$ is fixed, the hyperparameters $\boldsymbol{\Theta}_0$ is updated by maximizing $L(q^{old}(\hat{\boldsymbol{S}}), q(\boldsymbol{\Theta}_0))$, which is regarded as the expectation step. OG-WVBL solves sparse vectors by maximizing the lower bound $L(q(\boldsymbol{\Theta}))$, avoiding calculating the marginal likelihood function.

To facilitate the optimization of $L(q(\boldsymbol{\Theta}))$, the unknown probability distribution $q(\boldsymbol{\Theta})$ is factorized by using the mean field approximation of VBL [41]:

$$q(\boldsymbol{\Theta}) = q(\hat{\boldsymbol{S}})q(\nu_0)q(\boldsymbol{\nu})q(\boldsymbol{\beta}) \tag{20}$$

An alternating fashion for each latent variable can be expressed as [41]:

$$\ln q(\Theta_k) = E[\ln q(\bar{\boldsymbol{X}}, \Theta_k)_{q(\boldsymbol{\Theta}\setminus\Theta_k)}] + const \tag{21}$$

where $\boldsymbol{\Theta}\setminus\Theta_k$ denotes the set $\boldsymbol{\Theta}$ without Θ_k. The additive constant in (21) can be commonly obtained through normalization by

$$q_i(\Theta_i) = \frac{\exp(E[\ln p(\bar{\boldsymbol{X}}, \boldsymbol{\Theta})]_{j\neq i})}{\int \exp(E[\ln p(\bar{\boldsymbol{X}}, \boldsymbol{\Theta})]_{j\neq i})\mathrm{d}\Theta_i} \tag{22}$$

Since the numerical integration in the denominator is generally intractable, we choose conjugate prior distributions for each latent variables. According to (21) and the corresponding priori knowledge, EM rules is applied to each latent variable.

1) UPDATE OF $\hat{S}$

$$\begin{aligned}
&\ln q_{\hat{\boldsymbol{S}}}(\hat{\boldsymbol{s}}(t)) \\
&\quad = E[\ln(p(\bar{\boldsymbol{x}}(t)|\hat{\boldsymbol{s}}(t))p(\hat{\boldsymbol{s}}(t)|\boldsymbol{\nu}))]_{q_{\boldsymbol{\nu}}(\boldsymbol{\nu})q_{\nu_0}(\nu_0)} + const \\
&\quad \propto E[-\nu_0(\bar{\boldsymbol{x}}(t) - \boldsymbol{\Phi}(\boldsymbol{\beta})\hat{\boldsymbol{s}}(t))^{\mathrm{H}}(\bar{\boldsymbol{x}}(t) - \boldsymbol{\Phi}(\boldsymbol{\beta})\hat{\boldsymbol{s}}(t)) \\
&\qquad - \hat{\boldsymbol{s}}^{\mathrm{H}}(t)\boldsymbol{\Lambda}\hat{\boldsymbol{s}}(t)] \\
&\quad \propto E[-\hat{\boldsymbol{s}}^{\mathrm{H}}(t)(\nu_0\boldsymbol{\Phi}^{\mathrm{H}}(\boldsymbol{\beta})\boldsymbol{\Phi}(\boldsymbol{\beta}) + \boldsymbol{\Lambda})\hat{\boldsymbol{s}}(t) \\
&\qquad + \nu_0(\hat{\boldsymbol{s}}^{\mathrm{H}}(t)\boldsymbol{\Phi}^{\mathrm{H}}(\boldsymbol{\beta})\bar{\boldsymbol{x}}(t) + \bar{\boldsymbol{x}}^{\mathrm{H}}(t)\boldsymbol{\Phi}(\boldsymbol{\beta})\hat{\boldsymbol{s}}(t))]
\end{aligned} \tag{23}$$

From (23), it can be deduced that $\hat{\boldsymbol{s}}(t)$ follows a complex Gaussian distribution

$$q_{\hat{\boldsymbol{S}}}(\hat{\boldsymbol{s}}(t)) = CN(\hat{\boldsymbol{s}}(t)|\bar{\boldsymbol{\mu}}(t), \bar{\boldsymbol{\Sigma}}) \tag{24}$$

with its mean $\bar{\boldsymbol{\mu}}(t)$ and covariance matrix $\bar{\boldsymbol{\Sigma}}$ given as

$$\bar{\boldsymbol{\mu}}(t) = \nu_0\bar{\boldsymbol{\Sigma}}\boldsymbol{\Phi}^{\mathrm{H}}(\boldsymbol{\beta})\bar{\boldsymbol{x}}(t) \tag{25}$$

$$\bar{\boldsymbol{\Sigma}} = (\nu_0\boldsymbol{\Phi}^{\mathrm{H}}(\boldsymbol{\beta})\boldsymbol{\Phi}(\boldsymbol{\beta}) + \boldsymbol{\Lambda})^{-1} \tag{26}$$

Note that $\bar{\boldsymbol{\mu}}(t)$ and $\bar{\boldsymbol{\Sigma}}$ are the optimal posterior mean and covariance of $\hat{\boldsymbol{s}}(t)$. Therefore, $\bar{\boldsymbol{\mu}}(t), t = 1, 2, \cdots, T$ is used to update $\hat{\boldsymbol{S}}$:

$$\hat{\boldsymbol{S}} = [\bar{\boldsymbol{\mu}}(1), \bar{\boldsymbol{\mu}}(2), \cdots, \bar{\boldsymbol{\mu}}(T)] \tag{27}$$

2) UPDATE OF $\boldsymbol{\nu}$

Similarly, for the variational inference, the approximate posterior $q_{\boldsymbol{\nu}}(\boldsymbol{\nu})$ can be obtained as

$$\begin{aligned}
&\ln q_{\nu_n}(\nu_n) \\
&\quad = E[\ln(\prod_{t=1}^{T} p(\hat{s}_n(t)|\nu_n)p(\nu_n))]_{q_{\hat{\boldsymbol{S}}}(\hat{\boldsymbol{S}})q_{\nu_0}(\nu_0)}) + const \\
&\quad \propto E[(T + 2(c_n - 1))\ln\nu_n \\
&\qquad - (2d_n + \sum_{t=1}^{T}(\|\bar{\mu}_n(t)\|_2^2 + \bar{\Sigma}_{nn}))\nu_n]
\end{aligned} \tag{28}$$

According to (28), the posterior of ν_n follows a Gamma distribution.

$$q_{\nu_n}(\nu_n) = \Gamma(T + 2c_n - 1, 2d_n + \sum_{t=1}^{T}(\|\bar{\mu}_n(t)\|_2^2 + \bar{\Sigma}_{nn})) \tag{29}$$

Therefore, ν_n can be updated by its derivatives:

$$\nu_n^{new} = \frac{T + 2c_n - 2}{\sum_{t=1}^{T}(\|\bar{\mu}_n(t)\|_2^2 + \bar{\Sigma}_{nn}) + 2d_n} \tag{30}$$

3) UPDATE OF ν_0

The posterior distribution of noise precision ν_0 can be similarly updated as:

$$\begin{aligned}
&\ln q_{\nu_0}(\nu_0) \\
&= E[\ln(\prod_{t=1}^{T} p(\bar{\boldsymbol{x}}(t)|\hat{\boldsymbol{s}}(t), \nu_0)p(\nu_0))]_{q_{\hat{\boldsymbol{S}}}(\hat{\boldsymbol{S}})q_{\boldsymbol{\nu}}(\boldsymbol{\nu})})] + const \\
&\propto E[(TM + 2a - 2)\ln\nu_0 \\
&\quad - (2b + \sum_{t=1}^{T}(\|\bar{\boldsymbol{x}}(t) - \boldsymbol{\Phi}(\boldsymbol{\beta})\bar{\boldsymbol{\mu}}(t)\|_2^2 + \mathrm{tr}(\boldsymbol{\Phi}^{\mathrm{H}}(\boldsymbol{\beta})\boldsymbol{\Phi}(\boldsymbol{\beta})\bar{\boldsymbol{\Sigma}})))\nu_0]
\end{aligned} \tag{31}$$

According to (31), the posterior of ν_0 follows a Gamma distribution.

$$\begin{aligned}
q_{\nu_0}(\nu_0) = \Gamma(&TM + 2a - 1, \\
&2b + \sum_{t=1}^{T}(\|\bar{\boldsymbol{x}}(t) - \boldsymbol{\Phi}(\boldsymbol{\beta})\bar{\boldsymbol{\mu}}(t)\|_2^2 + \mathrm{tr}(\boldsymbol{\Phi}^{\mathrm{H}}(\boldsymbol{\beta})\boldsymbol{\Phi}(\boldsymbol{\beta})\bar{\boldsymbol{\Sigma}}))
\end{aligned} \tag{32}$$

The noise precision ν_0 for the optimized observation $\bar{\boldsymbol{X}}$ is updated by:

$$\nu_0^{new} = \frac{TM + 2a - 2}{2b + \sum_{t=1}^{T}(\|\bar{\boldsymbol{x}}(t) - \boldsymbol{\Phi}(\boldsymbol{\beta})\bar{\boldsymbol{\mu}}(t)\|_2^2 + \mathrm{tr}(\boldsymbol{\Phi}^{\mathrm{H}}(\boldsymbol{\beta})\boldsymbol{\Phi}(\boldsymbol{\beta})\bar{\boldsymbol{\Sigma}})} \tag{33}$$

For $\boldsymbol{\beta}$, it maximizes (21) is equivalent to minimizing the following expression:

$$E[\frac{1}{T}\sum_{t=1}^{T}\|\bar{\boldsymbol{x}}(t) - (\boldsymbol{A} + \boldsymbol{B}diag(\boldsymbol{\beta}))\hat{\boldsymbol{s}}(t)\|_2^2]$$

$$= \frac{1}{T}\sum_{t=1}^{T}\|\bar{\boldsymbol{x}}(t) - (\boldsymbol{A} + \boldsymbol{B}diag(\boldsymbol{\beta}))\hat{\boldsymbol{s}}(t)\|_2^2 + Tr\{(\boldsymbol{A} + \boldsymbol{B}diag(\boldsymbol{\beta}))\bar{\boldsymbol{\Sigma}}(\boldsymbol{A} + \boldsymbol{B}diag(\boldsymbol{\beta}))^{\mathrm{H}}\} = \boldsymbol{\beta}^{\mathrm{T}}\boldsymbol{P}_{\boldsymbol{\beta}}\boldsymbol{\beta} - 2\boldsymbol{\kappa}^{\mathrm{T}}\boldsymbol{\beta} + C \quad (34)$$

where C is a constant term, $\boldsymbol{P}_{\boldsymbol{\beta}}$ is a positive semidefinite matrix.

$$\boldsymbol{P}_{\boldsymbol{\beta}} = \Re\{\overline{\boldsymbol{B}^{\mathrm{H}}\boldsymbol{B}} \odot (\frac{1}{T}\sum_{t=1}^{T}\bar{\boldsymbol{\mu}}(t)\bar{\boldsymbol{\mu}}^{\mathrm{H}}(t) + \bar{\boldsymbol{\Sigma}})\} \quad (35)$$

$$\boldsymbol{\kappa} = \Re\{\frac{1}{T}\sum_{t=1}^{T}diag(\overline{\bar{\boldsymbol{\mu}}(t)})\boldsymbol{B}^{\mathrm{H}}(\bar{\boldsymbol{x}}(t) - \boldsymbol{A}\bar{\boldsymbol{\mu}}(t))\} - \Re\{diag(\boldsymbol{B}^{\mathrm{H}}\boldsymbol{A}\bar{\boldsymbol{\Sigma}})\} \quad (36)$$

where $\overline{\boldsymbol{B}^{\mathrm{H}}\boldsymbol{B}}$ is the complex conjugate. Because a closed-form expression of $\boldsymbol{\beta}$ cannot be given, we can get

$$\boldsymbol{\beta}^{new} = \arg\min_{\boldsymbol{\beta}\in[-\frac{1}{2}r,\frac{1}{2}r]^N}\{\boldsymbol{\beta}^{\mathrm{T}}\boldsymbol{P}_{\boldsymbol{\beta}}\boldsymbol{\beta} - 2\boldsymbol{\kappa}^{\mathrm{T}}\boldsymbol{\beta}\} \quad (37)$$

For VBL, the lower bound $L(q(\boldsymbol{\Theta}))$ [42] is used as the convergence criterion to accelerate the convergence speed and ensure the effectiveness of OG-WVBL.

$$L(q(\boldsymbol{\Theta})) \propto E[\ln(p(\bar{\boldsymbol{x}}(t)|\hat{\boldsymbol{s}}(t))] + E[\ln p(\hat{\boldsymbol{s}}(t)|\boldsymbol{v}))] + E[\ln p(\boldsymbol{v}))] + E[\ln p(v_0))] - E[\ln q(\hat{\boldsymbol{s}}(t))] - E[\ln q(\boldsymbol{v}))] - E[\ln q(v_0))] \quad (38)$$

B. UPDATE W PROCEDURE FOR OG-WVBL

As an alternate process, we update the outliers $\boldsymbol{W}$ while considering the hidden variable $\hat{\boldsymbol{S}}$ as a fixed sparse matrix. As is shown in Fig.1, the signal model is represented as:

$$\tilde{\boldsymbol{X}} = \boldsymbol{X} - \boldsymbol{\Phi}(\boldsymbol{\beta})\hat{\boldsymbol{S}} = \boldsymbol{W} + \tilde{\boldsymbol{E}} \quad (39)$$

It is clear that the dense Gaussian noise matrix $\tilde{\boldsymbol{E}}$ is equivalent to $\bar{\boldsymbol{E}}$ in (9). However, the noise precision v_0 of $\bar{\boldsymbol{E}}$ is relevant to $\hat{\boldsymbol{S}}$. Therefore, we employ a distinct hyperparameter ξ_0 to derive the outliers $\boldsymbol{W}$ instead of v_0:

$$p(\tilde{\boldsymbol{E}}|\xi_0) = \sum_{t=1}^{T}CN(\tilde{\boldsymbol{e}}(t)|\boldsymbol{0}, \xi_0^{-1}\boldsymbol{I}) \quad (40)$$

The hyperparameter ξ_0 is usually unknown in practice. A Gamma hyperprior for ξ_0 is similar to v_0:

$$p(\xi_0; a, b) = \Gamma(\xi_0|a, b) \quad (41)$$

The entries of the outliers $\boldsymbol{W}$ are sparse distribution. A few elements possess large amplitudes, however, most of the elements approach zero. There is no correlation between elements over time which means that $\boldsymbol{W}$ is not rows sparsity. The hierarchical prior model of $\hat{\boldsymbol{S}}$ can not be directly employed for $\boldsymbol{W}$. We assume that each element has independent statistics that can follow an IID Gaussian prior distribution with hyperparameter matrix $\boldsymbol{\xi}$, i.e.,

$$p(\boldsymbol{W}|\boldsymbol{\xi}) = \sum_{m=1}^{M}\sum_{t=1}^{T}CN(w_m(t)|0, \xi_{mt}^{-1}) \quad (42)$$

The hyperparameter ξ_{mt} is modeled as independent Gamma distribution with different weighted parameters e_{mt} and f_{mt}, i.e.,

$$p(\boldsymbol{\xi}; \boldsymbol{e}, \boldsymbol{f}) = \sum_{m=1}^{M}\sum_{t=1}^{T}\Gamma(\xi_{mt}|e_{mt}, f_{mt}) \quad (43)$$

Each element ξ_{mt} has different posterior because it is not fixed. Without loss of generality, the distribution (42) is a general expression of the one (13) so that it can handle different forms of $\boldsymbol{W}$. If there is impulsive noise arriving at time t, the elements in the tth column of $\boldsymbol{\xi}$ will be automatically occupied by outliers. In this case, since each hyperparameter ξ_{mt} has a different Gamma distribution, it is reasonable to give each ξ_{mt} different Gamma parameters, which can guarantee the accuracy of DOA estimation. Then, we have

$$p(\tilde{\boldsymbol{X}}|\boldsymbol{W}, \xi_0) = \sum_{t=1}^{T}CN(\tilde{\boldsymbol{x}}(t)|\boldsymbol{w}(t), \xi_0^{-1}\boldsymbol{I}) \quad (44)$$

where $\tilde{\boldsymbol{x}}(t)$ and $\boldsymbol{w}(t)$ denote the tth column of $\tilde{\boldsymbol{X}}$ and $\boldsymbol{W}$, respectively.

Similarly, for the variational inference, EM methodology is alternatively applied to update parameters $\{\boldsymbol{W}, \boldsymbol{\xi}, \xi_0\}$.

1) UPDATE OF W

The posterior distribution of hidden variables $\boldsymbol{W}$ can be updated as:

$$\begin{aligned}\ln q_{\boldsymbol{W}}(\boldsymbol{w}(t)) &= E[\ln(p(\tilde{\boldsymbol{x}}(t)|\boldsymbol{w}(t))p(\boldsymbol{w}(t)|\boldsymbol{\xi}_t))]_{q_{\xi_t}(\xi_t)q_{\xi_0}(\xi_0)} + const\\ &\propto E[-\xi_0(\tilde{\boldsymbol{x}}(t) - \boldsymbol{w}(t))^{\mathrm{H}}(\tilde{\boldsymbol{x}}(t) - \boldsymbol{w}(t)) - \boldsymbol{w}^{\mathrm{H}}(t)diag(\boldsymbol{\xi}_t)\boldsymbol{w}(t)]\\ &\propto E[-\boldsymbol{w}^{\mathrm{H}}(t)(\xi_0\boldsymbol{I}_M + diag(\boldsymbol{\xi}_t))\boldsymbol{w}(t) + \xi_0(\boldsymbol{w}^{\mathrm{H}}(t)\tilde{\boldsymbol{x}}(t) + \tilde{\boldsymbol{x}}^{\mathrm{H}}(t)\boldsymbol{w}(t))]\end{aligned} \quad (45)$$

From (45), it can be deduced that $\boldsymbol{w}(t)$ follows a complex Gaussian distribution. Then, the posterior distribution of outliers $\boldsymbol{W}$ is:

$$q_{\boldsymbol{W}}(\boldsymbol{w}(t)) = \sum_{t=1}^{T}CN(\boldsymbol{w}(t)|\tilde{\boldsymbol{\mu}}(t), \tilde{\boldsymbol{\Sigma}}(t)) \quad (46)$$

where

$$\tilde{\boldsymbol{\mu}}(t) = \xi_0\tilde{\boldsymbol{\Sigma}}(t)\boldsymbol{w}(t) \quad (47)$$

$$\tilde{\boldsymbol{\Sigma}}(t) = (\xi_0\boldsymbol{I}_M + diag(\boldsymbol{\xi}_t))^{-1} \quad (48)$$

The $\boldsymbol{W}$ is updated by:

$$\boldsymbol{W} = [\tilde{\boldsymbol{\mu}}(1), \tilde{\boldsymbol{\mu}}(2), \cdots, \tilde{\boldsymbol{\mu}}(T)] \quad (49)$$

2) UPDATE OF ξ

Similarly, the approximate posterior $q_{\boldsymbol{\xi}}(\boldsymbol{\xi})$ can be obtained as:

$$\begin{aligned}\ln q_{\xi_{mt}}(\xi_{mt}) &= E[\ln(p(\boldsymbol{w}_m(t)|\xi_{mt})p(\xi_{mt}))]_{q_{\boldsymbol{W}}(\boldsymbol{W})q_{\xi_0}(\xi_0)} + const\\ &\propto E[(2e_{mt} - 1)\ln\xi_{mt} - (2f_{mt} + \|\tilde{\mu}_m(t)\|_2^2 + (\xi_0 + \xi_{mt})^{-1})\xi_{mt}]\end{aligned} \quad (50)$$

From the above equation, the posterior of ξ_{mt} follows a Gamma distribution, that is

$$q_{\xi_{mt}}(\xi_{mt}) = \Gamma(2e_{mt}, 2f_{mt} + \|\tilde{\mu}_m(t)\|_2^2 + (\xi_0 + \xi_{mt})^{-1}) \quad (51)$$

Therefore, ξ_{mt} can be updated by its derivatives:

$$\xi_{mt}^{new} = \frac{2e_{mt} - 1}{2f_{mt} + \|\tilde{\mu}_m(t)\|_2^2 + (\xi_0 + \xi_{mt})^{-1}} \quad (52)$$

3) UPDATE OF ξ_0

The variational optimization of $q_{\xi_0}(\xi_0)$ yields

$$\begin{aligned} &\ln q_{\xi_0}(\xi_0) \\ &= E[\ln(\prod_{t=1}^{T} p(\tilde{\boldsymbol{x}}(t)|\boldsymbol{w}(t), \xi_0)p(\xi_0))]_{q_{\boldsymbol{W}}(\boldsymbol{W})q_{\boldsymbol{\xi}}(\boldsymbol{\xi})} + const \\ &\propto E[(TM+2a-2)\ln\xi_0 \\ &\quad - (2b+\sum_{t=1}^{T}\|\tilde{\boldsymbol{x}}(t)-\tilde{\boldsymbol{\mu}}(t)\|_2^2+\sum_{t=1}^{T}\sum_{m=1}^{M}(\xi_0+\xi_{mt})^{-1})\xi_0] \end{aligned} \quad (53)$$

From the above equation, the posterior of ξ_0 follows a Gamma distribution, that is

$$\begin{aligned} q_{\xi_0}(\xi_0) = \Gamma(&TM + 2a - 1, \\ &2b+\sum_{t=1}^{T}\|\tilde{\boldsymbol{x}}(t)-\tilde{\boldsymbol{\mu}}(t)\|_2^2+\sum_{t=1}^{T}\sum_{m=1}^{M}(\xi_0+\xi_{mt})^{-1}) \end{aligned} \quad (54)$$

Following the similar evidence procedure for updating ν_0, the hyperparameters ξ_0 is updated as:

$$\xi_0^{new} = \frac{TM+2a-2}{2b+\sum_{t=1}^{T}\|\tilde{\boldsymbol{x}}(t)-\tilde{\boldsymbol{\mu}}(t)\|_2^2+\sum_{t=1}^{T}\sum_{m=1}^{M}(\xi_0+\xi_{mt})^{-1}} \quad (55)$$

The properties of variational Bayesian learning guarantee the convergence of these parameters, as well as, the Kullback-Leibler divergence decreases continuously with the iteration process.

C. ITERATIVE REWEIGHTED STRATEGY

Typically, the goal of OG-WVBL is formulated as searching the optimal hyperparameters of $\boldsymbol{\nu}$ and $\boldsymbol{\xi}$ with the minimum number of non-zero entries. OG-WVBL applies different prior distributions to each element of sparse vectors by means of the iterative reweighted strategy, thus ensuring that the sparse model is consistent with the actual signal model. The iterative reweighted strategy of OG-WVBL eliminates the mutual influence of different signal components, and the reconstruction accuracy of each sparse vector is improved in the process of signal reconstruction. Compared with OGSBL [46], VBL is combined with the iterative reweighted strategy in this paper. OG-WVBL adjusts the iterative reweighted strategy by the sparse result of VBL, and control the priori distribution of hyperparameters of VBL by the iterative reweighted strategy. In the variational Bayesian learning, the sparse entries of $\hat{\boldsymbol{S}}$ and $\boldsymbol{W}$ is usually assumed the same probability distribution which means that they employ the same hyperparameters of ν_n and ξ_{mt}. However, we realize that only a few of $\hat{\boldsymbol{S}}$ and $\boldsymbol{W}$ is non-zero entries, and most entries close to zero [40]. In particular, there are very few non-zero entries with large amplitudes in $\boldsymbol{W}$. So giving more importance to those hyperparameters with non-zero entries over others, the different hyperparameters are assigned to the sparse entries of $\hat{\boldsymbol{S}}$ and $\boldsymbol{W}$ that encourage sparsity. The reweighted vector and VBL are updated alternately to promote convergence. With the iterative reweighted property, OG-WVBL can automatically identify the number of sources without any prior knowledge.

Assume that two reweighted vectors $\boldsymbol{\omega}$ and $\boldsymbol{\Delta}$ are used to represent $\hat{\boldsymbol{S}}$ and $\boldsymbol{W}$, respectively. If ω_n or Δ_{mt} holds a relatively large value, $\hat{\boldsymbol{S}}_n$ and W_{mt} will be non-zero. Usually, we can set $c_n = 1/\omega_n$, $d_n = \omega_n$, $e_{mt} = 1/\Delta_{mt}$, and $f_{mt} = \Delta_{mt}$. For the sake of simplicity, we will only analyze the relationship between $\boldsymbol{\omega}$ and $\hat{\boldsymbol{S}}$. If ω_n holds a relatively large value, the pdf of ν_n will be concentrated around zero which means that ν_n will reach to zero with higher probability, thus corresponding $\hat{\boldsymbol{S}}_n$ is non-zero with higher probability. Otherwise, if ω_n holds a small value, the pdf of ν_n is concentrated around its single mode ($\frac{1-\omega_n}{\omega_n^2} \approx \frac{1}{\omega_n^2}$), thus corresponding $\hat{\boldsymbol{S}}_n$ is zero with higher probability. We can choose a threshold η which ranges between 0 and $\frac{1}{\hat{\omega}^2}$ to differentiate between zero and non-zero element ν_n where $\hat{\omega}$ is the smallest entry of $\boldsymbol{\omega}$. With a suitable threshold, it is easy to identify the number of sources corresponding to the number of non-zero values in $\hat{\boldsymbol{S}}$. In the traditional VBL algorithm, the convergent hyperparameter ν_n possesses a large interval with zero element $\hat{\boldsymbol{S}}_n$. It is

Algorithm 1 Off-Grid Iterative Reweighted Variational Bayesian Learning

1) Input: $\boldsymbol{X}$, $\boldsymbol{\Phi}(\boldsymbol{\theta})$
2) Initialization: Set $\nu_0^0 = \xi_0^0 = 1$, $\boldsymbol{\nu}^0 = \frac{1}{\hat{\omega}^2}_{N\times 1}$, $\boldsymbol{\xi}^0 = \frac{1}{\hat{\boldsymbol{\Delta}}^2}_{M\times T}$, $\hat{\boldsymbol{S}}^0 = \boldsymbol{0}_{N\times T}$, $\boldsymbol{W}^0 = \boldsymbol{0}_{M\times T}$, $a = 1.0001$, $b = 10^{-4}$, $\varepsilon = 10^{-3}$, $h = 0$
3) While not converge do the following:
   a) Calculate $\bar{\boldsymbol{X}} = \boldsymbol{X} - \boldsymbol{W}^h$ according to (9)
   b) Calculate $\bar{\boldsymbol{\mu}}(t)$ and $\bar{\boldsymbol{\Sigma}}$ by (25) and (26), respectively
   c) Update ν_0^{h+1} and $\boldsymbol{\nu}^{h+1}$ using (33) and (30), respectively
   d) Update $\hat{\boldsymbol{S}}^{h+1} = [\bar{\boldsymbol{\mu}}(1), \bar{\boldsymbol{\mu}}(2), \cdots, \bar{\boldsymbol{\mu}}(T)]$ and $\boldsymbol{\omega}$
   e) Calculate $\tilde{\boldsymbol{X}} = \boldsymbol{X} - \boldsymbol{\Phi}(\boldsymbol{\beta})\hat{\boldsymbol{S}}^{h+1}$ according to (39)
   f) Calculate $\tilde{\boldsymbol{\mu}}(t)$ and $\tilde{\boldsymbol{\Sigma}}$ by (47) and (48), respectively
   g) Update ξ_0^{h+1} and $\boldsymbol{\xi}^{h+1}$ using (54) and (52), respectively
   h) Update $\boldsymbol{W}^{h+1} = [\tilde{\boldsymbol{\mu}}(1), \tilde{\boldsymbol{\mu}}(2), \cdots, \tilde{\boldsymbol{\mu}}(T)]$ and $\boldsymbol{\Delta}$
   i) Let iteration $h = h + 1$ and continue (goto Step-3a) until $\|L(q(\boldsymbol{\Theta}))^h - L(q(\boldsymbol{\Theta}))^{h-1}\|_2 / \|L(q(\boldsymbol{\Theta}))^{h-1}\|_2 < \varepsilon$
4) Output: $\hat{\boldsymbol{S}}^h$ and $\boldsymbol{W}^h$

difficult for the traditional VBL to select a suitable threshold to distinguish between zero and non-zero element ν_n.

Initially, the hyperparameters $\boldsymbol{\nu}$ and $\boldsymbol{\xi}$ are set to $\frac{1}{\hat{\omega}^2}$ and $\frac{1}{\hat{\Delta}^2}$. Usually, the reweighted vector $\boldsymbol{\omega}$ and $\boldsymbol{\Delta}$ comprise of 0.1 and 1 [40]. Therefore, in order to obtain a broad prior over the hyperparameters, all elements of $\boldsymbol{\omega}$ and $\boldsymbol{\Delta}$ are set to larger values. Therefore, we can obtain a broad prior over the hyperparameters. Of course, if some rough estimations of $\hat{\boldsymbol{S}}$ can be held, we set element ω_n to 0.1 with large value $\hat{\boldsymbol{S}}_n$. We can update the reweighted vector $\boldsymbol{\omega}$ and $\boldsymbol{\Delta}$ with a posteriori value $\hat{\boldsymbol{S}}$ in (27) and $\boldsymbol{W}$ in (49) to adjust the parameters of Gamma function, then the hyperparameters $\boldsymbol{\nu}$ and $\boldsymbol{\xi}$ are automatically adjusted. Therefore, the reweighted vector can promote convergence speed of OG-WVBL, and ensures that OG-WVBL can accurately estimate the number of sources without requiring the prior knowledge of sources. For clarity, we summarize our algorithm as *ALGORITHM*.

D. ANALYSIS OF PERFORMANCE

The computational complexity of $\bar{\boldsymbol{\Sigma}}$ and $\tilde{\boldsymbol{\Sigma}}$ in each iteration with Woodbury matrix identity are $O(MN^2)$ and $O(TM)$, respectively. The computational complexity of $\bar{\boldsymbol{\mu}}(t)$ and $\tilde{\boldsymbol{\mu}}(t)$ in each iteration are $O(TN^2)$ and $O(TM^2)$, respectively. The hyperparameters ν_0 and ξ_0 in each iteration need $O(TMN)$ and $O(TM)$ operations, respectively. The hyperparameters $\boldsymbol{\nu}$ and $\boldsymbol{\xi}$ in each iteration need $O(TN)$ and $O(TM)$ operations, respectively. Thus, the whole computational complexity is $O(MN^2 + TN^2 + TMN + TM^2)$.

IV. EXPERIMENT

A. IMPULSIVE NOISE MODE AND PERFORMANCE PARAMETER

In this experiment, we compare the performance of OG-WVBL, OGVBL, OGSBL [46], OGSBI [33], conventional VBL [42], FLOM-MUSIC [17], and l_p-MUSIC [11], as well as CRLB. OGVBL, which does not use the reweighted parameter, is a simplified version of OG-WVBL. We evaluate the performance of those algorithms from several aspects, namely, spectrum, convergence characteristic $\boldsymbol{\nu}$, generalized signal-to-noise ratio (GSNR), different characteristic exponents of α-stable distribution, angular separation of two direction angles, and grid interval. The FLOM-MUSIC and l_p-MUSIC adopt both 0.2° resolution of grid with MUSIC algorithm. Then, FLOM-MUSIC and l_p-MUSIC use the same fractional lower-order moments $p = 1.2$ to achieve a robust estimation. The emitting sources are two independent acoustic sources. The linear array is set to $M = 8$ omnidirectional acoustics sensors which are placed in half of the wavelength at the center frequency of the signal. The two sources impinging on the array from directions $\theta_1 = -16°$ and $\theta_2 = 15°$. The symmetric α-stable distribution ($S\alpha S$) is used to model impulsive noise. In every experiment, 2000 Monte-Carlo (MC) runs are performed.

Impulsive noise is usually expressed as the symmetric α-stable distribution. Its characteristic function is defined as:

$$\phi(t) = \exp(-\gamma|t|^{\alpha}) \tag{56}$$

where α is the characteristic exponent which describes the tails of the distribution with intervals ($0 \leq \alpha < 2$). Moreover, the smaller α becomes, the more impulsive will non-Gaussian noise be. γ is the dispersion. When characteristic $\alpha = 2$, it reduces to the Gaussian distribution. Since the second-order and higher-order moments of $S\alpha S$ are infinite for $\alpha < 2$, the common signal noise ratio (SNR) is meaningless. To quantify the relative strength between signal and impulsive noise, a generalized SNR (GSNR) can be expressed as:

$$GSNR = E[|s(n)|^2]/\gamma^{\alpha} \tag{57}$$

RMSE is the deviation criterion between observation and true value and can be given by:

$$RMSE = \sqrt{\frac{\sum_{l=1}^{L}(\hat{\theta}_1(l) - \theta_1)^2 + \sum_{l=1}^{L}(\hat{\theta}_2(l) - \theta_2)^2}{2L}} \tag{58}$$

where L represents the total number of MC run. $\hat{\theta}_1(l)$ and $\hat{\theta}_2(l)$ are the estimations of θ_1 and θ_2 in the MC run, respectively.

The resolution probability is that the two sources are resolvable if $\max_{p=1,2}\{\hat{\theta}_p - \theta_p\} < |\theta_1 - \theta_2|/2$.

Kozick has come to a closed-form expression of CRLB for impulsive noise [15], which can be expressed as:

$$C\ RLB = \frac{1}{I_c}\{\sum_{t=1}^{T} \Re[\boldsymbol{S}_d^{\mathrm{H}}(t)\boldsymbol{D}^{\mathrm{H}}(\boldsymbol{I} - \boldsymbol{A}(\boldsymbol{A}^{\mathrm{H}}\boldsymbol{A})^{-1}\boldsymbol{A}^{\mathrm{H}})\boldsymbol{D}\boldsymbol{S}_d(t)]\}^{-1} \tag{59}$$

where $\boldsymbol{S}_d(t) = diag(\boldsymbol{s}_1(t), \boldsymbol{s}_2(t), \cdots, \boldsymbol{s}_P(t))$ is a diagonal matrix of the received signal, $\boldsymbol{D} = [\frac{\partial \boldsymbol{a}(\theta_1)}{\partial \theta_1}, \cdots, \frac{\partial \boldsymbol{a}(\theta_P)}{\partial \theta_P}]$ is the differential of the array manifolds $\boldsymbol{A}$. The coefficient I_c can be expressed as $I_c = \int_0^{\infty} \frac{(f'(x))^2}{f(x)} x dx$ where $x = |n|$ is the modulus of impulsive noise. $f(x)$ is pdf of x. Note that $I_1 = \frac{1}{2\gamma}$ with $\alpha = 1$ and $I_2 = \frac{3}{5\gamma^2}$ with $\alpha = 2$. For simplicity, the coefficient I_c for $1 < \alpha < 2$ can be approximated by first order linear interpolation with I_1 and I_2 [11] .

B. CONVERGENCE OF HYPERPARAMETERS

Fig.4 shows that hyperparameters $\boldsymbol{\nu}$ of OGSBL, OGVBL and OG-WVBL after convergence where $\alpha = 1.4$, $GSNR = 8$ and snapshots $T = 100$. In order to get the prior reweighted vector $\boldsymbol{\omega}$, MUSIC algorithm was used to estimate $\hat{\boldsymbol{S}}$ based on 20 snapshots in each trial. It can be easily seen that the hyperparameter ν_n can take any value in OGSBL and OGVBL after convergence. Consequently, it is difficult to select a suitable threshold to distinguish between zero and non-zero elements ν_n. However, most values ν_n of OG-WVBL are concentrated around 100 corresponding to $\hat{\boldsymbol{S}}_n$ will be considered as zero. With a suitable threshold such as $\eta = 1$, OG-WVBL is easier to identify the number of sources than OGSBL and OGVBL

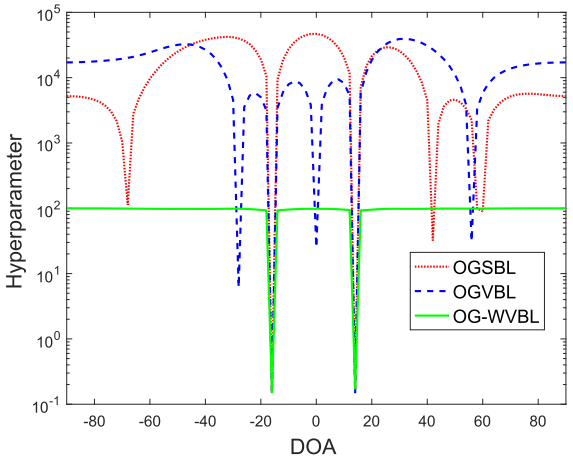

FIGURE 4. The values of hyperparameters v after convergence for OG-WVBL, OGVBL, and OGSBL algorithms.

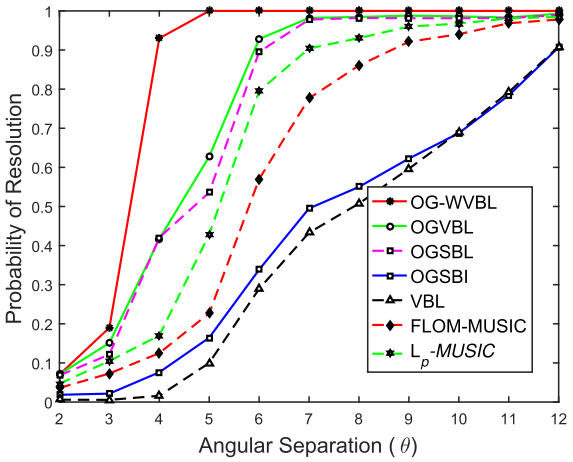

FIGURE 6. The probability of resolution of different algorithms in $S\alpha S$ noise versus angular separation.

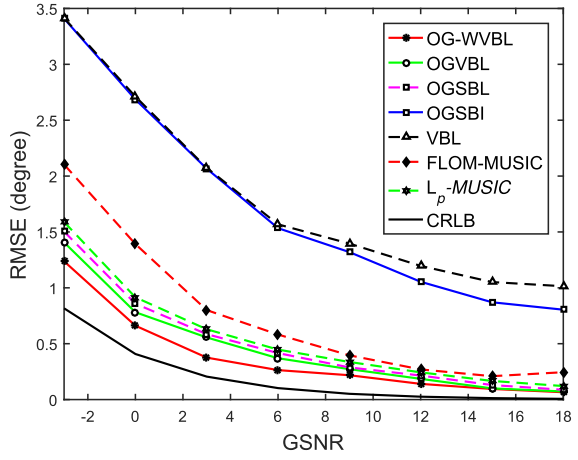

FIGURE 5. The RMSE comparison of different algorithms in $S\alpha S$ noise versus GSNR.

which is based on a unified assumption with respect to the hyperparameters. Therefore, OG-WVBL can reach perfect performance than OGSBL and OGVBL at relatively low GSNR.

C. PERFORMANCE COMPARISON

Figs.5 analyzes the RMSE of the DOA estimation of different algorithms in $S\alpha S$ noise versus GSNR where $\alpha = 1.5$ and snapshots $T = 200$. The performance of those algorithms is improved as GSNR increases. Besides, OG-WVBL achieves a smaller reconstruction error in comparison with OGSBL and OGVBL as GSNR decreases. Thus, OG-WVBL will remain stable in low GSNR. When $GSNR = 12$, all algorithms are close to the approximated CRLB, that is, impulsive noise has little effect on the performance except OGSBI and VBL. The traditional OGSBI and VBL almost fail to reconstruct the sparse signal in low GSNR.

Fig.6 depicts the performance of different algorithms when DOA of the second source is gradually away from that of the first source where $\alpha = 1.5$, $GSNR = 8$ and snapshots $T = 200$. The first DOA is $\theta_1 = -16°$. As expected, the OG-WVBL can effectively differentiate the two sources with 5° angle separation. Furthermore, OG-WVBL requires a smaller angle separation threshold than other algorithms associated with a fixed probability of resolution. OGSBL and OGVBL also exhibit excellent performance in dealing with impulsive noise. However, the performance of VBL and OGSBI is relatively poor because they have no ability to suppress impulsive noise.

In this simulation, we aim at evaluating the performance of the characteristic exponent α on the basis of RMSE where $GSNR = 8$ and snapshots $T = 200$. As was mentioned before, the heavy tails of impulsive noise are controlled by the characteristic exponent α. It is clear from Fig.7 that the RMSE of these algorithms decreases as α increases. OG-WVBL which is based on a heavy-tailed distribution achieves a better reconstruction performance, when compared with OGSBI and VBL. Moreover, the smaller α becomes, the worse will the performance of OGSBI and VBL be. When the characteristic exponent α is 2, noise follows Gaussian distribution and all algorithms can achieve better performance.

Fig.8 and Fig.9 show that the performance of different algorithms in $S\alpha S$ noise versus grid intervals where $\alpha = 1.5$, $GSNR = 8$ and snapshots $T = 200$. With the increase of grid interval, OGSBI and VBL have a poor performance on describing the true observation model. OG-WVBL has a relatively stable RMSE which means that OG-WVBL results in a much accurate solution and a low complexity when working in a coarse grid. The computational time of OG-WVBL will slightly decrease as grid interval increases because the complexity of updating the outliers $\boldsymbol{W}$ remains constant. Because OGVBL adopts two iterative VBL, its complexity is greater than that of OGSBI. Owing to the weighted strategy, OG-WVBL needs less iteration after convergence, so that, it requires less computational time than OGSBL and OGVBL.

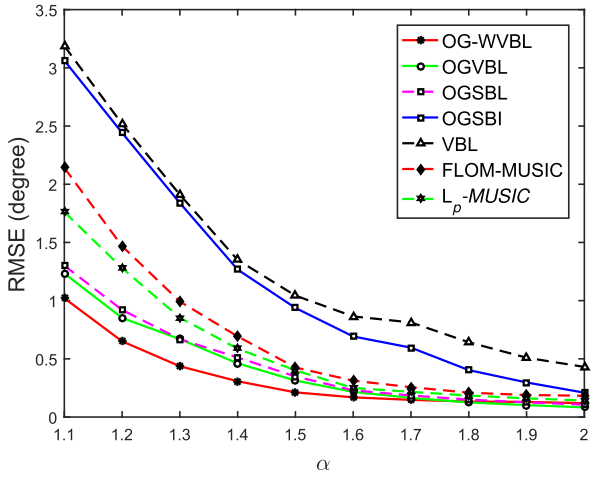

FIGURE 7. The RMSE comparison of different algorithms in $S\alpha S$ noise versus characteristic exponent α.

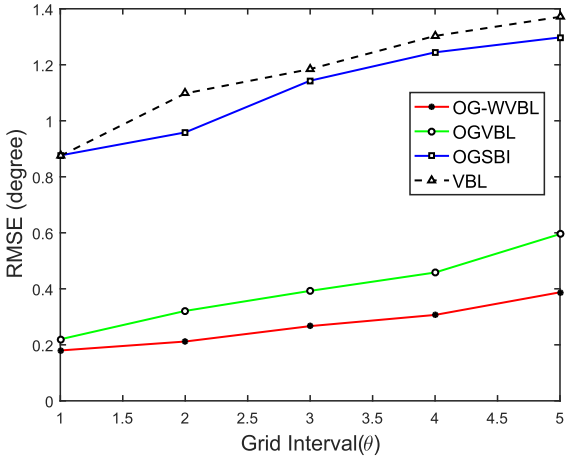

FIGURE 8. The RMSE comparison of different algorithms in $S\alpha S$ noise versus grid interval.

Above simulation results show that the proposed algorithm is valid for the sparse signal recovery in the presence of the $S\alpha S$ noise.

D. DEMONSTRATION OF TRUCK SYSTEM

In order to evaluate the stability performance, we perform three independent trials in impulsive noise environment with three trucks. From Fig.10, three standard truck sources are produced from Bluetooth speakers which are located at $[-16°, 0°, 15°]$. Impulsive noise is composed of the noise of machine, equipment startup, instantaneous attack of heavy objects, blast of wind, clapping and so on which can refer to Fig.1. The grid interval is set to 2° for OG-WVBL and OGSBI. We employ three segment data where each segment composed of 1000 samplings. Fig.11 shows that the OGSBI can not accurately estimate DOA every trial, and the performance severely degrades in impulsive noise environment. However, OG-WVBL is less sensitive to impulsive noise

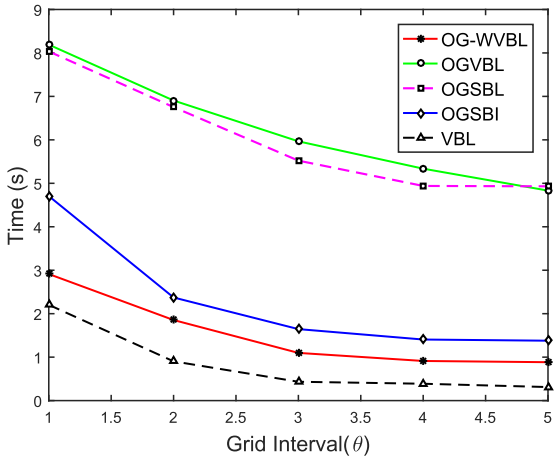

FIGURE 9. The computational time comparison of different algorithms in $S\alpha S$ noise versus grid interval.

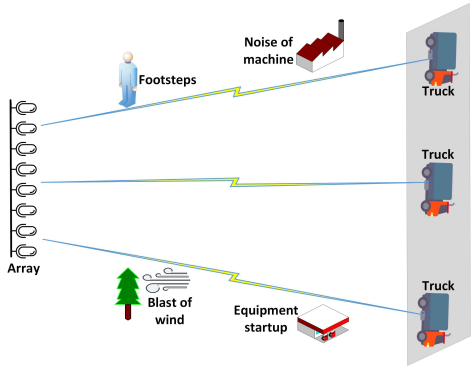

FIGURE 10. Acoustic array scenario with impulsive noise environment, $M = 8$.

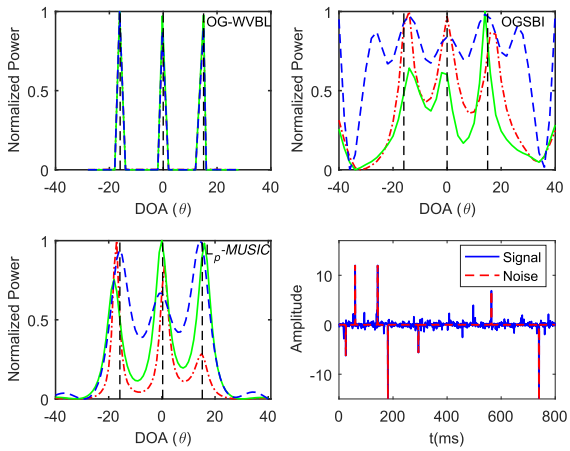

FIGURE 11. Spatial spectrum of three independent trials in impulsive noise environment with three truck, $M = 8$.

every trial. At the same time, the originally received data of the reference sensor is displayed with one of experiments and the location of impulsive noise is estimated by OG-WVBL at the last figure of Fig.11. The impulsive noise comes from

420-455ms data of Fig.1. It can be seen that the OG-WVBL can also effectively identify the impulsive noise.

V. CONCLUSION

In this paper, we propose a method of sparse representation for highly impulsive noise with heavy tails, based on a variational Bayesian learning framework. Impulsive noise in truck environment is modeled as α-stable distribution. OG-WVBL employs impulsive noise as two independent components, and models directly the outliers with sparse distribution in time domain. OG-WVBL utilizes two iterative VBL to reconstruct signal and outliers matrix and then retrieves the DOA. OG-WVBL also introduces the reweighted vector to hyperparameters so that the more importance is given to those hyperparameters with non-zero entries over others which can encourage sparsity. The experiments and simulation results show that OG-WVBL possesses robust performance and outperforms several existing algorithms under the impulsive noise environment. Because the heavy tails of impulsive noise can be treated as a sparse matrix, OG-WVBL is not only suitable for α-stable distribution, but also can effectively deal with other impulsive noise models.

ACKNOWLEDGMENT

Fuqiang Ma and Cheng Xu are co-first authors and contribute equally to this work.

REFERENCES

[1] J. Xie, L. Wang, and Y. Wang, "Efficient real-valued rank reduction algorithm for DOA estimation of noncircular sources under mutual coupling," *IEEE Access*, vol. 6, pp. 64450–64460, 2018.

[2] E. D. Di Claudio, R. Parisi, and G. Jacovitti, "Space time MUSIC: Consistent signal subspace estimation for wideband sensor arrays," *IEEE Trans. Signal Process.*, vol. 66, no. 10, pp. 2685–2699, May 2018.

[3] A. Das, "A Bayesian sparse-plus-low-rank matrix decomposition method for direction-of-arrival tracking," *IEEE Sensors J.*, vol. 17, no. 15, pp. 4894–4902, Aug. 2017.

[4] F. Ma and X. Zhang, "Wideband DOA estimation based on focusing signal subspace," *Signal, Image Video Process.*, vol. 13, no. 4, pp. 675–682, 2019.

[5] R. O. Schmidt, "Multiple emitter location and signal parameter estimation," *IEEE Trans. Antennas Propag.*, vol. AP-34, no. 3, pp. 276–280, Mar. 1986.

[6] R. Roy and T. Kailath, "Esprit-estimation of signal parameters via rotational invariance techniques," *IEEE Trans. Acoust., Speech, Signal Process.*, vol. 37, no. 7, pp. 984–995, Jul. 1989.

[7] F.- G. Yan, Y. Shen, and M. Jin, "Fast DOA estimation based on a split subspace decomposition on the array covariance matrix," *Signal Process.*, vol. 115, pp. 1–8, Oct. 2015.

[8] M. R. Anbiyaei, W. Liu, and D. C. McLernon, "Performance improvement for wideband DOA estimation with white noise reduction based on uniform linear arrays," in *Proc. IEEE Sensor Array Multichannel Signal Process. Workshop (SAM)*, Jul. 2016, pp. 1–5.

[9] L. Lu and H. Zhao, "Active impulsive noise control using maximum correntropy with adaptive kernel size," *Mech. Syst. Signal Process.*, vol. 87, pp. 180–191, Mar. 2017.

[10] A. M. Zoubir, V. Koivunen, Y. Chakhchoukh, and M. Muma, "Robust estimation in signal processing: A tutorial-style treatment of fundamental concepts," *IEEE Signal Process. Mag.*, vol. 29, no. 4, pp. 61–80, Jul. 2012.

[11] W.-J. Zeng, H. C. So, and L. Huang, "ℓ_p-MUSIC: Robust direction-of-arrival estimator for impulsive noise environments," *IEEE Trans. Signal Process.*, vol. 61, no. 17, pp. 4296–4308, Sep. 2013.

[12] M. Novey, T. Adali, and A. Roy, "A complex generalized Gaussian distribution—Characterization, generation, and estimation," *IEEE Trans. Signal Process.*, vol. 58, no. 3, pp. 1427–1433, Mar. 2010.

[13] C. L. Nikias and M. Shao, *Signal Processing With Alpha-Stable Distributions and Applications*. Hoboken, NJ, USA: Wiley, 1995.

[14] J. Shang, Z. Wang, and Q. Huang, "A robust algorithm for joint sparse recovery in presence of impulsive noise," *IEEE Signal Process. Lett.*, vol. 22, no. 8, pp. 1166–1170, Aug. 2015.

[15] R. J. Kozick and B. M. Sadler, "Maximum-likelihood array processing in non-Gaussian noise with Gaussian mixtures," *IEEE Trans. Signal Process.*, vol. 48, no. 12, pp. 3520–3535, Dec. 2000.

[16] P. Tsakalides and C. L. Nikias, "The robust covariation-based MUSIC (ROC-MUSIC) algorithm for bearing estimation in impulsive noise environments," *IEEE Trans. Signal Process.*, vol. 44, no. 7, pp. 1623–1633, Jul. 1996.

[17] T.-H. Liu and J. M. Mendel, "A subspace-based direction finding algorithm using fractional lower order statistics," *IEEE Trans. Signal Process.*, vol. 49, no. 8, pp. 1605–1613, Aug. 2001.

[18] H. Belkacemi and S. Marcos, "Robust subspace-based algorithms for joint angle/Doppler estimation in non-Gaussian clutter," *Signal Process.*, vol. 87, no. 7, pp. 1547–1558, 2007.

[19] A. Swami and B. M. Sadler, "On some detection and estimation problems in heavy-tailed noise," *Signal Process.*, vol. 82, no. 12, pp. 1829–1846, Dec. 2002.

[20] M. Muma, Y. Cheng, F. Roemer, M. Haardt, and A. M. Zoubir, "Robust source number enumeration for R-dimensional arrays in case of brief sensor failures," in *Proc. IEEE Int. Conf. Acoust., Speech Signal Process. (ICASSP)*, Mar. 2012, pp. 3709–3712.

[21] M. Salibián-Barrera, S. Van Aelst, and G. Willems, "Principal components analysis based on multivariate MM estimators with fast and robust bootstrap," *J. Amer. Stat. Assoc.*, vol. 101, no. 475, pp. 1198–1211, 2006.

[22] J. Dai, X. Xu, and D. Zhao, "Direction-of-arrival estimation via real-valued sparse representation," *IEEE Antennas Wireless Propag. Lett.*, vol. 12, pp. 376–379, 2013.

[23] N. Hu, Z. Ye, X. Xu, and M. Bao, "DOA estimation for sparse array via sparse signal reconstruction," *IEEE Trans. Aerosp. Electron. Syst.*, vol. 49, no. 2, pp. 760–773, Apr. 2013.

[24] M. Carlin, P. Rocca, G. Oliveri, F. Viani, and A. Massa, "Directions-of-arrival estimation through Bayesian compressive sensing strategies," *IEEE Trans. Antennas Propag.*, vol. 61, no. 7, pp. 3828–3838, Jul. 2013.

[25] J. Yin and T. Chen, "Direction-of-arrival estimation using a sparse representation of array covariance vectors," *IEEE Trans. Signal Process.*, vol. 59, no. 9, pp. 4489–4493, Sep. 2011.

[26] M. E. Tipping, "Sparse Bayesian learning and the relevance vector machine," *J. Mach. Learn. Res.*, vol. 1, pp. 211–244, Sep. 2001.

[27] S. Ji, Y. Xue, and L. Carin, "Bayesian compressive sensing," *IEEE Trans. Signal Process.*, vol. 56, no. 6, p. 2346, 2008.

[28] L. Zhao, G. Bi, L. Wang, and H. Zhang, "An improved auto-calibration algorithm based on sparse Bayesian learning framework," *IEEE Signal Process. Lett.*, vol. 20, no. 9, pp. 889–892, Sep. 2013.

[29] Z.-M. Liu and Y.-Y. Zhou, "A unified framework and sparse Bayesian perspective for direction-of-arrival estimation in the presence of array imperfections," *IEEE Trans. Signal Process.*, vol. 61, no. 15, pp. 3786–3798, Aug. 2013.

[30] Q. Huang, G. Zhang, and Y. Fang, "Real-valued DOA estimation for spherical arrays using sparse Bayesian learning," *Signal Process.*, vol. 125, pp. 79–86, Aug. 2016.

[31] N. Hu, B. Sun, J. Wang, J. Dai, and C. Chang, "Source localization for sparse array using nonnegative sparse Bayesian learning," *Signal Process.*, vol. 127, pp. 37–43, Oct. 2016.

[32] S. S. Chen, D. L. Donoho, and M. A. Saunders, "Atomic decomposition by basis pursuit," *SIAM Rev.*, vol. 43, no. 1, pp. 129–159, 2001.

[33] Z. Yang, L. Xie, and C. Zhang, "Off-grid direction of arrival estimation using sparse Bayesian inference," *IEEE Trans. Signal Process.*, vol. 61, no. 1, pp. 38–43, Jan. 2013.

[34] Y. Zhang, Z. Ye, X. Xu, and N. Hu, "Off-grid DOA estimation using array covariance matrix and block-sparse Bayesian learning," *Signal Process.*, vol. 98, no. 1, pp. 197–201, May 2014.

[35] J. Dai, X. Bao, W. Xu, and C. Chang, "Root sparse Bayesian learning for off-grid DOA estimation," *IEEE Signal Process. Lett.*, vol. 24, no. 1, pp. 46–50, Jan. 2017.

[36] A. Koochakzadeh and P. Pal, "On saturation of the Cramér Rao bound for sparse Bayesian learning," in *Proc. IEEE Int. Conf. Acoust., Speech Signal Process. (ICASSP)*, Mar. 2017, pp. 3081–3085.

[37] Y. Bian, "Polarimetric SAR statistical analysis using alpha-stable distribution and its application in optimal despeckling," *Int. J. Remote Sens.*, vol. 34, no. 19, pp. 6796–6836, Jun. 2013.
[38] D. Xiao, T. He, Q. Pan, X. Liu, and Y. Shan, "Impulsive noise cancellation of acoustic emission signal based on iterative mathematical morphology filter," *J. Vibroengineering*, vol. 15, no. 4, pp. 1752–1764, 2013.
[39] J. Lin, M. Nassar, and B. L. Evans, "Impulsive noise mitigation in powerline communications using sparse Bayesian learning," 2013, *arXiv:1303.1217*. [Online]. Available: https://arxiv.org/abs/1303.1217
[40] A. Al Hilli, L. Najafizadeh, and A. Petropulu, "Weighted sparse Bayesian learning (WSBL) for basis selection in linear underdetermined systems," in *Proc. 4th Int. Workshop Compressed Sens. Theory Appl. Radar, Sonar Remote Sens. (CoSeRa)*, Sep. 2016, pp. 115–119.
[41] D. G. Tzikas, A. C. Likas, and N. P. Galatsanos, "The variational approximation for Bayesian inference," *IEEE Signal Process. Mag.*, vol. 25, no. 6, pp. 131–146, Jan. 2008.
[42] C. M. Bishop and M. E. Tipping, "Variational relevance vector machines," in *Proc. 6th Conf. Uncertainty Artif. Intell.* Burlington, MA, USA: Morgan Kaufmann, 2000, pp. 46–53.
[43] K. Yang, Y. Zhang, Z. Lei, and R. Duan, "Direction of arrival estimation in linear arrays with intersubarray displacement errors using sparse Bayesian inference," *IEEE Access*, vol. 6, pp. 67235–67243, 2018.
[44] L. Wang, L. Zhao, G. Bi, C. Wan, L. Zhang, and H. Zhang, "Novel wideband DOA estimation based on sparse Bayesian learning with Dirichlet process priors," *IEEE Trans. Signal Process.*, vol. 64, no. 2, pp. 275–289, Jan. 2016.
[45] K. Liu, J. Wang, Z. Xing, L. Yang, and J. Fang, "Low-rank phase retrieval via variational Bayesian learning," *IEEE Access*, vol. 7, pp. 5642–5648, 2019.
[46] J. Dai and H. C. So, "Sparse Bayesian learning approach for outlier-resistant direction-of-arrival estimation," *IEEE Trans. Signal Process.*, vol. 66, no. 3, pp. 744–756, Feb. 2018.

FUQIANG MA received the B.E. degree in computer science and technology from the University of Science and Technology Beijing, China, in 2015, where he is currently pursuing the Ph.D. degree. His research interests include wireless sensor networks, pattern recognition, array signal processing, and machine learning.

CHENG XU received the B.E., M.S., and Ph.D. degrees from the University of Science and Technology Beijing (USTB), China, in 2012, 2015, and 2019 respectively, where he is currently an Associate Professor with the Data and Cyber-Physical System Laboratory (DCPS). He was supported by the Postdoctoral Innovative Talent Support Program from Chinese Government. His research interests include swarm intelligence, multi-robots networks, wireless localization, and the Internet of Things.

XIAOTONG ZHANG received the M.E. and Ph.D. degrees from the University of Science and Technology Beijing, in 1997 and 2000, respectively, where he was a Professor with the Department of Computer Science and Technology. His industry experience includes affiliation with Beijing BM Electronics High-Technology Company Ltd., from 2002 to 2003, where he was involved in digital video broadcasting communication systems and IC design. His industrial cooperation experience includes BLX IC Design Company Ltd., North Communications Corporation of Petro, China, and Huawei Technologies Company Ltd.. His research interest includes the quality of wireless channels and networks, wireless sensor networks, networks management, cross-layer design and resource allocation of broadband and wireless networks, and the signal processing of communication and computer architecture.

JIE HE received the B.E. and Ph.D. degrees from the University of Science and Technology Beijing, Beijing, China, in 2005 and 2012, respectively, where he is currently an Associate Professor with the School of Computer and Communication Engineering and a Researcher of the Data and Cyber-Physical System Laboratory (DCPS). His current research interests include indoor location systems, wireless sensor networks, and body area networks.

WEI SU is currently pursuing the University of Science and Technology Beijing, China. His current research and academic interests focus on array sensor processing, spectrum analysis, and radio localization.